

Biointerface Research in Applied Chemistry

www.BiointerfaceResearch.com

<https://doi.org/10.33263/BRIAC96.547559>

Original Research Article

Open Access Journal

Received: 18.07.2019 / Revised: 16.10.2019 / Accepted: 17.10.2019 / Published on-line: 25.10.2019

Binuclear metal complexes of a symmetric polydentate donor hydrazone: synthesis, spectral characterization, DNP DFT computational and biological studies

Mohamed Gaber Abuelazm¹, Ola Ahmed El-Gammal^{2,*}, Sherif Abdelmoneam Mandour²

¹Faculty of Science, Chemistry Department, , Tanta University, Tanta, P.O.Box 70, Egypt.

²Department of Chemistry, Faculty of Science, Mansoura University, Mansoura, P.O.Box 70, Mansoura- Egypt

*corresponding author e-mail address: olaelgamma@yahoo.com

ABSTRACT

Co(II), Ni(II)and Cu(II) complexes of a new chelate namely 2,2'-(9S,10S,11R,12R)-9,10-dihydro-9,10-ethanoanthracene-11,12-dicarbonyl)bis(N-phenylhydrazine-1-carboxamide) (H₆EPH) were synthesized and were characterized by using analytical and spectral techniques suggesting tetrahedral geometry for Ni(II) and Cu(II) complexes and an octahedral for Co(II) complex. The ESR spectral data showed one broad band with $g \parallel > 2.0036$ indicating the axial symmetry with the unpaired electron residing in the $d_{x^2-y^2}$ orbital with appreciable covalent character of the metal-ligand bond. The molecular modeling a using DFT method was drawn and the bond lengths, bond angles, chemical reactivity and energy components (kcal/mol) for all the title compounds were evaluated. Also, all compounds were examined for DNA cleavage ability and antioxidant using superoxide dismutase like- activity.

Keywords: Binuclear, symmetric polydentate, spectral characterization; thermal degradation; and SOD anti-oxidant activities.

1. INTRODUCTION

Over last decades, there has been growing interest in the study of hydrazones as they constitute a versatile class of compounds within numerous chemical as well as pharmacological applications [1-3]. Many researches revealed that hydrazones possess antimicrobial, anticonvulsant, analgesic, and anticonvulsant, pharmacological and catalytic properties [4-6]. The aromatic hydrazone molecules dispersed in a binder polymer were utilized as the main constituent of electrophotographic photoreceptors of laser printers due to their excellent hole-transporting properties and relatively simple synthesis [7]. Also, some beneficial hydrazones such as hydrazone-based molecular glasses for solid-state dye-sensitized solar cells [8] and those as di-

2-pyridyl ketone benzoyl hydrazone (dpkbh) for the determination of trace amounts of metal ions in solutions have been widely developed [9,10]. Nowadays, antioxidants that show scavenging activities of superoxide radicals are increasingly receiving attention [11]. On continuation the work carried out earlier [12,13], we present herein synthesis and characterization of a new series of Co(II), Ni(II) and Cu(II) complexes that derived from 9S,10S,11R,12R)-9,10-dihydro-9,10-ethanoanthracene-11,12-dicarbonyl)bis(N-phenylhydrazicarbonoxyamide)(H₆EPH) as a novel hydrazone and testing their DNA cleavage and superoxide dismutase (SOD)-like activities.

2. MATERIALS AND METHODS

2.1. Materials and physical measurements.

All chemicals used were of Aldrich or Fluka grade. C, H and N percent were determined using a Perkin-Elmer 2400 series II analyzer. The chloride and metal contents were determined according to the standard methods. IR spectra (4000–400cm⁻¹) for KBr discs were recorded on a Mattson 5000 FTIR spectrophotometer. Unicam UV–Vis spectrophotometer UV2 was used for displaying the electronic spectra. Magnetic susceptibilities were measured with a Sherwood scientific magnetic susceptibility balance at 298 K. NMR spectra were measured using Varian V NMR 400 (¹H, 400 MHz; ¹³C, 101 MHz) spectrometer using CDCl₃, or DMSO-d₆ as a solvent and internal reference. Electrospray ionization (ESI) mass spectra were recorded on a Thermo Scientific (Rockford, IL, USA) Q Exactive (Orbitrap mass spectrometer). TGA, DTA measurements (20–800°C) were recorded on a DTG-50 Shimadzu thermogravimetric analyzer at a heating rate of 10 °C/min and nitrogen flow rate of 15 ml/min. A powder ESR spectrum was carried out in a 2 mm quartz capillary at room temperature with a Bruker EMX

spectrometer working in the X-band (9.78 GHz) with 100 kHz modulation frequency. XRD patterns were obtained using Philips X-ray diffractometer (model X'pert) with utilized monochromatic Cu Ka radiation operated at 40 kV and 30 mA and a scanning speed of 8 (deg /min) in the 2θ range 10°–80°.

2.2. Synthesis of 2,2'-(9S,10S,11R,12R)-9,10-dihydro-9,10-ethanoanthracene-11,12-dicarbonyl)bis(N-phenylhydrazine-1-carboxamide) (H₆EPH).

The ligand, H₆EPH (Scheme 1) was prepared by mixing 9, 10-dihydro-9, 10-ethanoanthracene-11, 12- diacidhydrazide [14] in a 1:2 molar ratio with phenyl isocyanate in 20 ml hot ethanolic solution. The reaction mixture was boiled under reflux for 6 h and remains in cold place overnight. The isolated white product was filtered off, recrystallized from absolute ethanol and finally dried in a vacuum desiccator over anhydrous calcium chloride and has been checked by TLC and characterized by elemental analysis (C, H, N and S) and spectral (IR, UV-Vis., ¹H NMR and mass).

2.3. Synthesis of metal complexes.

Hot ethanolic solution (20 ml) of the respective chloride salt (0.001 mol) was added to a hot

ethanolic suspension (20 ml) of the respective ligand (0.001 mol) with constant stirring. The reaction mixture was refluxed with constant stirring for 4 hours until a precipitate was formed immediately then filtered off, washed several times with hot ethanol and dried under vacuum anhydrous CaCl_2 . The physical and analytical data are listed in Table 1.

2.4. Computational details.

DMOL3 module calculations were used to examine the cluster estimations [15] and double numerical basis sets plus polarization functional (DNP) implemented in Materials Studio bundle [16]. It is designed for the realization of large scale density functional theory (DFT) calculations [17-20]. The geometric optimization is performed without any symmetry restriction.

2.5. Biological studies

2.5.1. DNA cleavage studies. This was carried out as described [21]. 20 mg DNA/methyl green (Sigma, St. Louis, MO, USA) was suspended in 100 ml of 0.05 M Tris-HCl buffer, pH 7.5, containing 7.5 mM MgSO_4 and stirred at 37°C with a magnetic

stirrer for 24 h. The ligand and its metal complexes were dissolved in EtOH in Eppendorf tubes. The solvent was removed under vacuum and 200 μl of the DNA/methyl green solution was added to each tube. The absorption maximum for the DNA/methyl green complex is 642.5-645 nm. Samples were incubated in the dark at ambient temperature. After 24 h, the final absorbance of samples was determined. Readings were corrected for initial absorbance and normalized as a % of the untreated DNA/methyl green absorbance value. IC_{50} 's were determined for each compound.

2.5.2. Superoxide dismutase (SOD) scavenging activity. Superoxide dismutase (SOD)-like activity was tested using Bridges and Salin method [22, 23]. This method is used on the basis of the inhibitory action of SOD on the reduction of nitroblue tetrazolium (NBT) by the superoxide anion produced by the xanthine / xanthine oxidase system. Free H_6EPH ligand solution or its metal complexes were prepared in dimethylsulphoxide (DMSO). For comparative intents, the activity of *L-Ascorbic acid* has also been determined.

Table 1. Analytical and physical data of H_6EPH and its complexes.

Compound	F.Wt	Color	Yield %	M.P., °C	Found (Calcd.) %				
					C	H	N	M	Cl
H_6EPH	560.61	white	85	275	68.57 (68.56)	5.35 (5.03)	14.5 (14.99)	---	---
$[\text{Co}_2(\text{H}_6\text{EPH})(\text{OH})_2(\text{H}_2\text{O})_4].5\text{H}_2\text{O}$	872.61	Pink	75	> 300	43.15 (44.05)	5.00 (5.31)	9.25 (9.63)	13.32 (13.51)	---
$[\text{Ni}_2(\text{H}_6\text{EPH})(\text{OH})_2(\text{H}_2\text{O})_2].4\text{H}_2\text{O}$	818.09	Pale green	80	> 300	47.46 (46.98)	5.69 (4.93)	9.91 (10.27)	14.85 (14.35)	---
$[\text{Cu}_2(\text{H}_6\text{EPH})(\text{Cl})_4].4\text{H}_2\text{O}$	883.55	Pale green	70	> 300	43.06 (43.50)	3.31 (3.88)	9.65 (9.51)	14.50 (14.38)	15.85 (16.05)

3. RESULTS

The complexes (figure 1b-1d) are insoluble either in water or in non-polar organic solvents but soluble in DMF and DMSO solvents. The molar conductivity value of all metal complexes ($\Omega=11-18 \text{ ohm}^{-1} \text{ cm}^2 \text{ mol}^{-1}$ in DMF) indicates nonelectrolytic nature [24]. Many attempts were done to grow up single crystals for the solid metal complexes but failed.

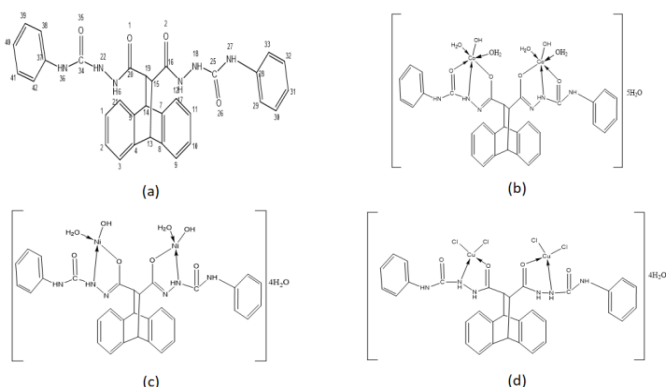


Figure 1. Structural representation of (a) H_6EPH , (b) $[\text{Co}_2(\text{H}_6\text{EPH})(\text{OH})_2(\text{H}_2\text{O})_4].5\text{H}_2\text{O}$, (c) $[\text{Ni}_2(\text{H}_6\text{EPH})(\text{OH})_2(\text{H}_2\text{O})_2].4\text{H}_2\text{O}$ and (d) $[\text{Cu}_2(\text{H}_6\text{EPH})(\text{Cl})_4].4\text{H}_2\text{O}$.

3.1. IR spectral studies.

The IR spectrum for H_6EPH (Fig. 1a) exhibits strong bands at 1745, 1699 and 1651 cm^{-1} attributable to hydrogen bonded, free carbonyl groups of hydrazone and $\nu(\text{C=O})_{\text{phenyl}}$, respectively [25]. This is confirmed by the broad band at 3461 cm^{-1} attributable to $\nu(\text{OH})$ in the spectrum. The bands at 3101, 3351 and 3323 assignable to $\nu(\text{N}^1\text{H})$, $\nu(\text{N}^4\text{H})$ and $\nu(\text{N}^2\text{H})$ modes [26] while those due to $\nu(\text{C=C})_{\text{phenyl}}$ and amide (I-III) vibrations are observed at 1604 cm^{-1} and {1540, 1322, and 928 cm^{-1} }. The later bands contain

substantial contributions from $\nu(\text{C=N})$, $\delta(\text{C-H})$ and $\delta(\text{N-H})$ vibrations [26]. The band appeared at 954 cm^{-1} is due to $\nu(\text{N-N})$. A comparison of the spectra of H_6EPH and its complexes (Error! Reference source not found.) reveals that the ligand coordinates in keto and enol forms. Firstly as neutral N_2O_2 tetradeятate in $[\text{Cu}_2(\text{H}_6\text{EPH})(\text{Cl})_4].4\text{H}_2\text{O}$ complex (Fig. 1d) (coordinating to both metal ions through two $(\text{C=O})_{\text{hydrazone}}$ and two N^2H groups confirmed by the blue shift of these groups to lower wave number also shift of $\nu(\text{N-N})$ to higher wavenumber as a result of contribution of azomethine group. Secondly, in $[\text{Co}_2(\text{H}_6\text{EPH})(\text{OH})_2(\text{H}_2\text{O})_4].5\text{H}_2\text{O}$ and $[\text{Ni}_2(\text{H}_6\text{EPH})(\text{OH})_2(\text{H}_2\text{O})_2].4\text{H}_2\text{O}$ complexes (Figs. 1b & 1c) the ligand reacts as dibasic hexadentate via two $[(\text{C-O})_{\text{hydrazone}}, \text{N}^2\text{H}$ and $(\text{C=O})_{\text{benzoyl}}$ formed after deprotonation of C-OH groups. This behaviour is confirmed by:

- Disappearance of bands due to $\nu(\text{C=O})_{\text{hydrazine}}$ and $\nu(\text{N}^1\text{H})$.
- The negative shift of $(\text{C=O})_{\text{phenyl}}$ suggesting its participation in coordination.
- The appearance of a new band at (1568 and 1547) and 1116 cm^{-1} assignable to $\nu(\text{C=N})$ [27] supporting the proposed mode of chelation.
- The new bands at 3400 and (1334-1339) cm^{-1} attributed to $\nu(\text{OH})$ and $\delta(\text{OH})$ confirm coordination through this group [27].

3.2. NMR spectra.

The ^1H NMR spectrum of the H_6EPH derivative in d_6 -DMSO (Fig. 2a) reveals signals at δ : 10.02, 9.29 and 9.26 ppm may be referred to N^4H , N^2H and N^1H protons, respectively [28]. These signals diminished on the addition of D_2O . The signals attributable to phenyl protons appear as two multiplets at δ : 7.01-7.06 & 7.15-7.28 ppm. Moreover, the protons of CH groups ($\text{CH}_13-\text{CH}_14$)

appear at 4.467, 3.41 ppm (dd, $J=3.60$, 1H) and (CH15-CH19) as a broad signal at 4.096 ppm. No signal appeared in the downfield region at 11-15 ppm. However, again the duplication of most signals are relevant to the existence of cis-trans isomerism. Also, the ^{13}C NMR Spectrum of the H₆EPH in d₆-DMSO (Fig. 2b) indicated signals for (C=O)_{hydrazone} and (C=O)_{benzoyl} observed at δ : 171.19 and 143.36 ppm [28] while those existed as two multiplets in the regions δ : 123.02-124.71 & 125.40-125.49 ppm are referred to phenyl carbons. Finally, the peaks observed as multiplet at (39.22, 39.50 ppm) and (40.06-40.42 ppm) are due to (C13-C14) and (C15-C19).

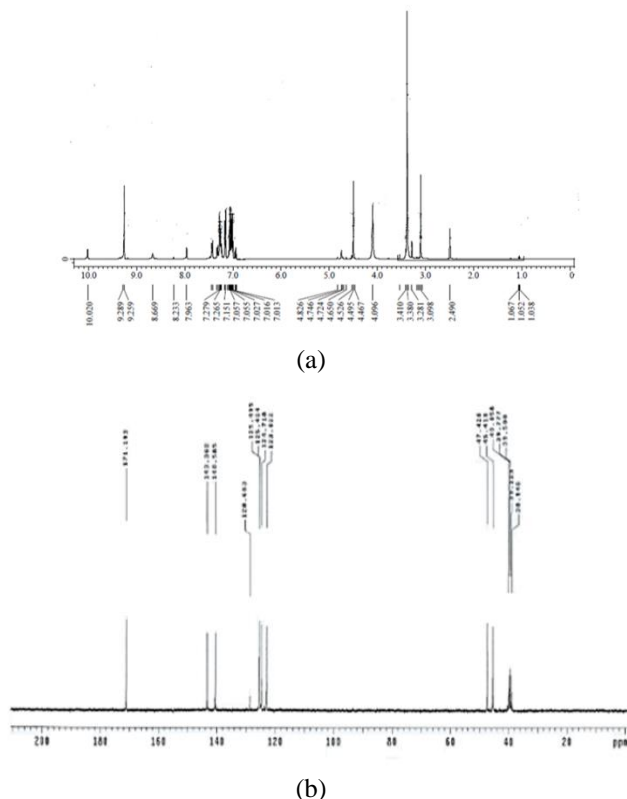


Figure 2. (a) ^1H -NMR and (b) ^{13}C -NMR spectra of H₆EPH in d₆-DMSO.

3.3. Electronic spectra and magnetic moments.

UV-Vis spectral absorption spectra of H₆EPH and its complexes were displayed in dimethylformamid (DMF) solution and the tentative assignments of the characteristic spectral absorption bands and magnetic moments of metal complexes are listed in table 3. The spectrum of H₆EPH exhibited bands at 42918–31847 and 24213–29411 cm⁻¹ assignable to ($\pi \rightarrow \pi^*$) and n \rightarrow π^* transitions of benzene ring and carbonyl groups. A large change occurs for

these bands on complexation with new bands appeared at 18939, 19841 and 19841 cm⁻¹ revealing the participation of NH group in complexation [29].

The M²⁺ \rightarrow Cl transition is generally found in the 27322–27932 cm⁻¹ region and would contribute to the higher energy n \rightarrow π^* band [30]. The band located at 23584–20833 cm⁻¹ in the spectra of the complexes may be due to LMCT. The green color and absorption bands in the electronic spectra of Ni(II) and Cu(II) complexes are consistent with the tetrahedral geometry. On the other hand the electronic spectrum of Co(II) complex suggests an octahedral structure. Also, the values of ligand field parameters (Dq, B and β) are 798.189 cm⁻¹, 913.94 cm⁻¹ and 0.9412 which are typical for octahedral Co²⁺ complexes [31]. The value of β indicates an appreciable degree of covalency of the Co(II) ligand bonds. Generally, the subnormal value of the magnetic moment values (2.80 B.M) per one atom reveals strong M-M interaction [31].

3.4. ESR spectra.

The room temperature solid state ESR spectrum of the binuclear [Cu₂(H₆EPH)(Cl)₄][.]4H₂O complex is represented in figure 3 indicating only an intense and broad signal with unresolved hyperfine couplings ($g_{iso}=2.083$). Such spectrum gives only one g value that arises from extensive exchange coupling through misalignment of the local molecular axes between different molecules in the unit cell (dipolar broadening) and enhanced spin lattice relaxation [32]. The higher g value for the investigated complex, when compared to that of free electron ($g=2.0023$) revealing an appreciable covalency of the metal ligand bonding with dx²-y² as the ground-state characteristic of tetrahedral stereochemistry [33].

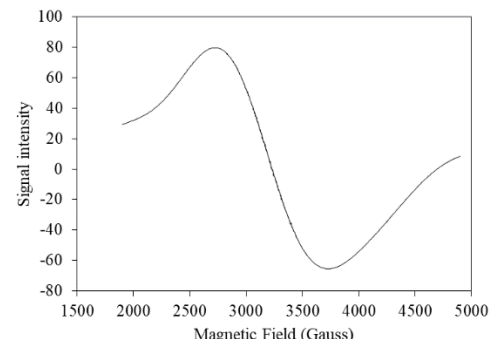


Figure 3. ESR spectrum of [Cu₂(H₆EPH)(Cl)₄][.]4H₂O complex.

Table 2. FT-IR spectral bands of H₆EPH and its metal complexes.

Compound	v(N ⁴ H)	v(N ² H)	v(N ¹ H)	v(N-N)	v(C=O) bonded	v(C=O) hy	v(C=O)ph	v(C=C)	v(C=N) _{azo}
H₆EPH	3351	3323	3101	1025	1745	1699 _w	1651	1604	1540
[Co ₂ (H ₄ EPH)(OH) ₂ (H ₂ O) ₄] [.] 5H ₂ O	3410	3227	--	1026	--	--	1641	1606	1538
[Ni ₂ (H ₄ EPH)(OH) ₂ (H ₂ O) ₂] [.] 4H ₂ O	3389	3279	--	1025	---	---	1648	1604	1568
[Cu ₂ (H ₆ EPH)(Cl) ₄] [.] 4H ₂ O	3336	3295	3176	1024	--	1706	1651	1630	1558

Table 3. Spectral absorption bands, magnetic moments and ligand field parameters of H₆EBT metal complexes.

Compound	μ_{eff} (B.M.)	Intraligand and d-d transition cm ⁻¹	Ligand field parameters		
			Dq (cm ⁻¹)	B (cm ⁻¹)	β
H₆EPH	-	42918, 31847, 26881, 24875, 20449, 19267	-	-	-
[Co ₂ (H ₄ EPH)(OH) ₂ (H ₂ O) ₄] [.] 5H ₂ O	2.06	42016, 37174, 29940, 26666, 22883, 16722, 14903	789.19	913.94	0.9412
[Ni ₂ (H ₄ EPH)(OH) ₂ (H ₂ O) ₂] [.] 4H ₂ O	1.56	41493, 35714, 25773, 22883, 21739, 19801, 17667	1016.27	803.98	0.772
[Cu ₂ (H ₆ EPH)(Cl) ₄] [.] 4H ₂ O	1.25	42553, 35211, 28735, 21413, 20964, 18518, 16666	-	-	-

3.5. Mass spectra

The mass spectra of H₆EPH is given in figure 4 that shows the molecular ion peak at m/z = 560.22 (23.40%) corresponding to C₃₂H₂₈N₆O₄ of the ligand. the fragmentation pattern of H₆EPH is given in figure 5.

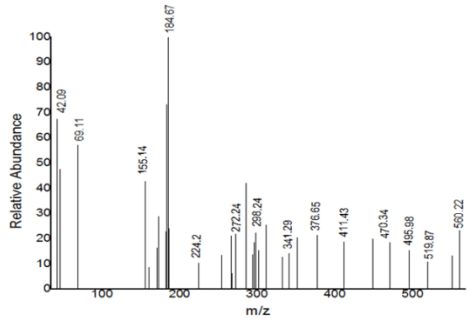


Figure 4. Mass spectrum of H₆EPH.

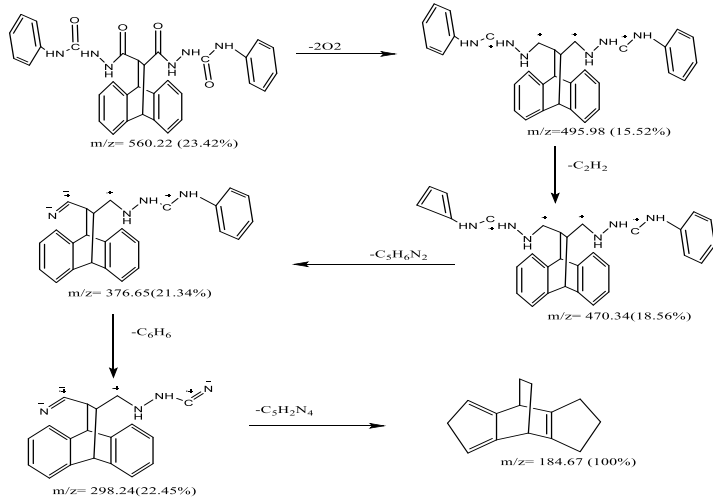


Figure 5. Schematic representation of fragmentation pattern of H₆EPH.

3.6. X Ray powder diffraction

The XRD pattern of the [Co₂(H₄EPH)(OH)₂(H₂O)₄]⁵H₂O complex is shown in figure 6. All of the diffraction peaks were perfectly indexed into the face centered monoclinic CoCl₂.2H₂O structures with lattice constant a=7.28, b=8.522, c= 3.573 Å and β= 97.55° and C2/m space group. This is in good agreement with the Joint Committee for Powder Diffraction Studies (JCPDS) File No. 3.786 [34].

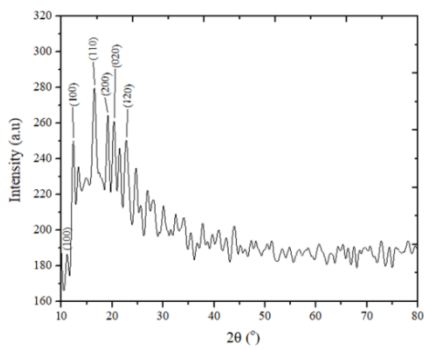


Figure 6. X-Ray powder diffraction for [Co₂(H₄EPH)(OH)₂(H₂O)₄]⁵H₂O complex.

No diffraction peaks are observed in the XRD spectrum attributed to nature structural of free ligand. This means that the free ligand of this Co (II) complex presented as amorphous form. Table 4

gives the peaks positions (2θ), miller indices (hkl) and the relative peaks intensities as well as the d-spacing of the material.

Table 4. XRD data of the isolated [Co₂(H₄EPH)(OH)₂(H₂O)₄]⁵H₂O and [Cr₂(H₄EPH)Cl₄]⁸H₂O complexes: the positions of the peaks (2θ), and its relative intensities (I/I₀) and, the d-spacing.

2θ(°)	hkl	I/I ₀ × 10 ²	d-spacing (Å)
11.01	(100)	2.31	8.03
12.40	(100)	3.04	7.13
16.51	(110)	3.44	5.36
19.17	(200)	3.71	4.62
20.38	(020)	3.68	4.35
22.57	(120)	3.30	3.93

3.7. Thermogravimetric studies.

The structural elucidation of the investigated complexes was further recognized by a careful examination of their thermogravimetric, TG patterns (Fig. 7). The data obtained listed in table 5 revealed good matchmaking between the chemical composition and the fragmentation pattern. TG of the ligand represented three decomposition stages while its metal complexes represented four or five decomposition stages. The first degradation stage in metal complexes generally occurred before 150° presumably due to loss of hydrated water and the residual part may be the metal or metal oxide.

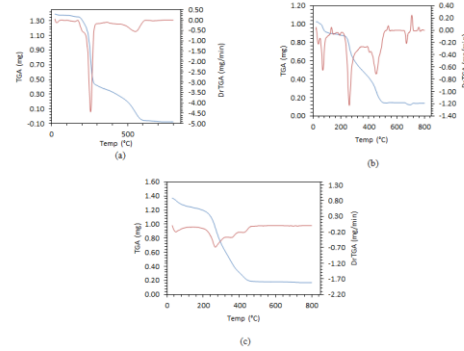


Figure 7. Thermal analysis curves (TGA, DTGA) of (a) H₆EPH, (b) [Co₂(H₄EPH)(OH)₂(H₂O)₄]⁵H₂O, (c) [Ni₂(H₄EPH)(OH)₂(H₂O)₂]⁴H₂O.

3.7.1. Kinetic Studies.

The kinetic parameters of decomposition stages have been evaluated by using non-isothermal methods namely, Coats-Redfern [35] and Horowitz-Metzger [36]. The data are summarized in tables 6 and 7. The data revealed the following remarks:

- The degradation steps which show a best fit for (n=1), suggesting a decomposition of first-order in all cases.
- The activation energy, (E_a), increases or decreases for the subsequent degradation steps according to the stability of the remaining species.
- The positive value of ΔG displayed that the rate of ligand removal will be lower from step to the subsequent step. This lowering may be occurred because the oversize structural rigidity of remaining complex after the removal of one or more ligand moieties [37].
- The positive values of entropy change of some complexes, may suggest that the disorder of the decomposed fragments increases much more rapidly than that of the undecomposed one [38].
- The positive value of ΔH* means the endothermic nature of the decomposition processes [39].

Table 5. Decomposition steps with the temperature range and weight loss for H₂DPD and its metal complexes.

Compound	step	Temp. range	(%calc) %Found	Species Removed
H₆EPH	1 st	182-223	(8.21) 8.736	-(H ₂ O+N ₂)
	2 nd	224-467	(56.57) 56.8	-(2C ₆ NHCO + C ₆ H ₄)
	3 rd	468-614	(22.60) 22.15	-(N ₂ +H ₂ O+C ₆ H ₈)
	Residue	615-800	(13.24) 13.31	6C
[Co₂(H₄EPH)(OH)₂(H₂O)₄].5H₂O	1 st	23- 50	(2.06) 2.06	-(H ₂ O)
	2 nd	51- 80	(8.26) 8.32	-(4H ₂ O)
	3 rd	81- 104	(4.12) 4.21	-(2H ₂ O)
	4 th	105- 414	(28.90) 27.95	-(2H ₂ O +2OH+2C ₆ H ₅ +N ₂)
	5 th	415- 480	(23.41) 23.97	-(C ₁₁ H ₁₆ N ₄)
	Residue	480-800	(33.22) 33.49	Co ₂ O ₄ +9C
[Ni₂(H₄EPH)(OH)₂(H₂O)₂].4H₂O	1 st	30- 77	(8.80) 9.80	- (4H ₂ O)
	2 nd	78- 322	(45.27) 45.92	-(2H ₂ O +2OH+C ₂₄ H ₁₈)
	3 rd	323-389	(20.79) 20.16	-(C ₄ H ₆ N ₆ O ₂)
	4 th	390-466	(10.77) 10.67	-(C ₄ H ₈ O ₂)
	Residue	467-800	(14.34) 13.45	2Ni

Table 6. Kinetic Parameters of complexes evaluated by Coats-Redfern equation.

Compound	Peak	Mid.Tem (K)	Ea kJ/mol	A (S-1)	ΔH* kJ/mol	ΔS* kJ/mol	ΔG* kJ/mol
H₆EPH	1 st	479.00	274.44	8.75×10 ²⁷	270.46	0.2861	133.44
	2 nd	527.43	336.96	4.75×10 ³¹	332.58	0.3568	144.41
	3 rd	812.69	606.75	6.50×10 ³⁷	600.00	0.4706	217.52
[Co₂(H₄EPH)(OH)₂(H₂O)₄].5H₂O	1 st	312.22	287.14	3.85×10 ⁴⁶	284.54	0.6465	82.68
	2 nd	343.13	229.12	1.31×10 ³³	226.27	0.3879	93.16
	3 rd	371.30	237.74	1.04×10 ³²	234.66	0.3662	98.70
	4 th	532.65	369.90	2.41×10 ³⁴	365.47	0.4085	147.91
	5 th	725.16	386.55	4.00×10 ²⁵	380.52	0.2378	280.05
[Ni₂(H₄EPH)(OH)₂(H₂O)₂].4H₂O	1 st	329.98	87.61	8.14×10 ¹¹	84.87	-0.0177	90.72
	2 nd	534.96	200.56	2.00×10 ¹⁷	196.11	0.0814	152.54
	3 rd	621.65	629.35	7.70×10 ⁴⁹	624.19	0.7040	186.54
	4 th	691.00	285.96	4.00×10 ¹⁹	280.22	0.1233	194.98
	5 th	479.00	274.44	8.75×10 ²⁷	270.46	0.2861	133.44

Table 7. Kinetic Parameters of complexes evaluated by Horowitz-Metzger equation.

Compound	Peak	Mid.Tem (K)	Ea kJ/mol	A (S-1)	ΔH* kJ/mol	ΔS* kJ/mol	ΔG* kJ/mol
H₆EPH	1 st	479.00	283.81	7.51×10 ²⁷	273.53	0.3259	137.81
	2 nd	527.43	343.09	3.45×10 ³¹	329.60	0.2634	139.72
	3 rd	812.69	599.90	4.65×10 ³⁷	602.86	0.5649	216.79
[Co₂(H₄EPH)(OH)₂(H₂O)₄].5H₂O	1 st	312.22	292.56	3.08×10 ⁴⁷	289.97	0.6638	82.71
	2 nd	343.13	232.67	4.43×10 ³³	229.82	0.3981	93.23
	3 rd	371.30	245.87	1.44×10 ³³	242.78	0.3880	98.71
	4 th	532.65	376.92	1.15×10 ³⁵	372.49	0.4215	148.00
	5 th	725.16	390.75	7.79×10 ²⁵	384.72	0.2434	208.24
[Ni₂(H₄EPH)(OH)₂(H₂O)₂].4H₂O	1 st	329.98	92.77	5.10×10 ¹²	90.02	-0.0025	90.84
	2 nd	534.96	205.87	6.32×10 ¹⁷	201.42	0.0910	152.74
	3 rd	621.65	608.21	1.31×10 ⁴⁸	603.04	0.6701	186.45
	4 th	691.00	299.00	3.80×10 ²⁰	293.26	0.1421	195.07
	5 th	479.00	283.81	7.51×10 ²⁷	273.53	0.3259	137.81

Table 8. Calculated E_{HOMO}, E_{LUMO}, energy band gap (E_H-E_L), electronegativity (χ), chemical potential (μ), global hardness (η), global softness (S), global electrophilicity index (ω) and softness (σ) of H₆EPH and its metal complexes.

Compound	E _H (eV)	E _L (eV)	(E _H -E _L) (eV)	X (eV)	μ (eV)	η (eV)	S (eV ⁻¹)	ω (eV)	σ (eV)
H₆EPH	-4.662	-1.227	-3.435	2.945	-2.945	1.718	0.859	2.524	0.582
[Co₂(H₄EPH)(OH)₂(H₂O)₄].5H₂O	-3.575	-2.131	-1.444	2.853	-2.853	0.722	0.361	5.637	1.385
[Ni₂(H₄EPH)(OH)₂(H₂O)₂].4H₂O	-3.933	-2.001	-1.932	2.967	-2.967	0.966	0.517	4.556	1.035
[Cu₂(H₆EPH)(Cl)₄].4H₂O	-5.242	-4.77	-0.472	5.006	-5.006	0.236	2.119	53.093	4.237

H: HOMO, L: LUMO.

3.8. DFT molecular modeling.

3.8.1. Geometry optimization using DFT study. The optimized structures as deduced from DFT using Materials Studio package for ligands and their complexes are shown in figure 8 and the

obtained data of bond lengths and angles are recorded in Table (1S-8S). The following remarks can be concluded;

- (i) The bond lengths and angles of both ligands are altered on metal chelation. The bond angles in Ni (II) and Cu (II) complexes

are consistent with that reported for tetrahedral complexes while for Co (II) they are similar to the octahedral complexes with sp^3 and sp^3d^2 hybrid orbitals [40].

(ii) All the bonds of the coordination sites become longer and weaker than that previously found in the ligand, H_6EPH (e.g. C-O, C-N bond distances) as a result of metal-oxygen, and metal-nitrogen bonds formation that results in the weakness of the carbon-nitrogen, and carbon-oxygen confirming the participation of C-O and C-N in complexation. There is a variation in N-N bond lengths of both ligands due to the coordination takes place via N atoms of the $(C=N)$ azomethine [40].

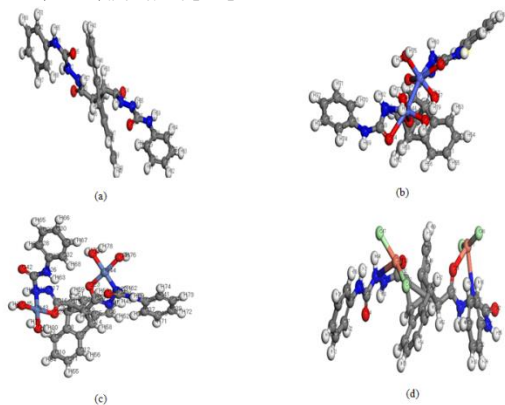


Figure 8. Optimized molecular structures of: (a) H_6EPH , (b) $[Co_2(H_4EPH)(OH)_2(H_2O)_4].5H_2O$, (c) $[Ni_2(H_4EPH)(OH)_2(H_2O)_2].4H_2O$ and (d) $[Cu_2(H_6EPH)(Cl)_4].4H_2O$.

3.8.2. Chemical reactivity descriptors. DFT method concept can indicate the chemical reactivity and site selectivity of the molecular systems. The energies of frontier molecular orbitals ($E_{HOMO}+E_{LUMO}$), energy band gap ($E_{HOMO}-E_{LUMO}$) which illustrate the resultant charge transfer interaction within the molecules, electronegativity (χ), chemical potential (μ), global hardness (η), global softness (S) and global electrophilicity index (ω) [41] are listed in table 8.

The obtained E_{HOMO} and E_{LUMO} (Figures 9 & 10) were negative indicating the stability of these compounds. A hard molecule is represented by large HOMO-LUMO difference while a soft and more active framework has a small energy difference. The importance of η and σ is to measure the molecular stability and reactivity. In a complex formation system, the ligand acts as a Lewis base while the metal ion acts as a Lewis acid. Metal ions are soft acids and thus soft base ligands are most effective for complex formation [42]. Also, the small optical energy gap, ($E_{HOMO} - E_{LUMO}$) for the hydrazone (-2.945ev) and its complexes suggest that charge transfer easily occurs in it which influences the biological activity of the molecule.

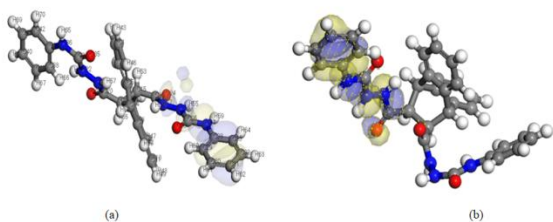


Figure 9. (a) HOMO (b) LUMO of H_6EPH ligand.

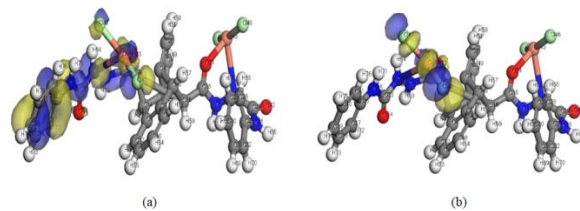


Figure 10. (a) HOMO (b) LUMO of $[Cu_2(H_6EPH)(Cl)_4].4H_2O$ complex.

3.9. Biological studies.

3.9.1. DNA cleavage studies. A colorimetric assay was used to measure the displacement of methyl green from DNA by compounds with the ability to bind to DNA. This was determined spectrophotometrically by a decrease in absorbance at 630 nm. An insight at figure 11 indicates that all compounds exhibited remarkable affinity towards DNA-binding whereas the hydrazone, H_6EPH is the most active compound with IC_{50} $35.6\pm2.0\mu\text{g/ml}$ and title compounds according to DNA-binding affinity follows the order: $H_6EPH > [Ni_2(H_4EPH)(OH)_2(H_2O)_2].4H_2O > [Co_2(H_4EPH)(OH)_2(H_2O)_4].5H_2O > [Cu_2(H_6EPH)(Cl)_4].4H_2O$. This was demonstrated either by retaining the DNA-compound complex at the origin or by migrating for very short distances [43].

3.9.2. Scavenging activities of superoxide radicals. Superoxide dismutase (SOD) is the first line of vindication against injury caused by reactive oxygen species (ROS), which catalyze the dismutation of O_2^- to H_2O_2 , and O_2 [44]. Therefore, It is important to find SOD mimics, which have SOD activity and provide stability. This work focused on the metal dependent SOD mimics, their assays, chemical characters and usage.

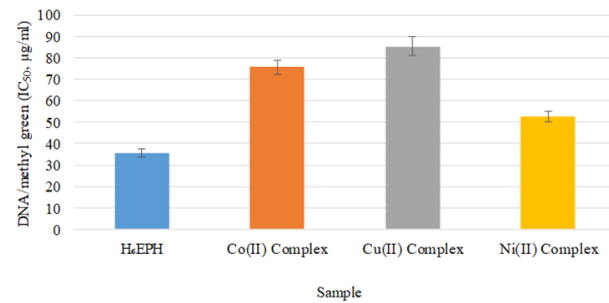


Figure 11. DNA/methyl green $IC_{50}\mu\text{g/ml}$ of H_6EPH and its metal complexes.

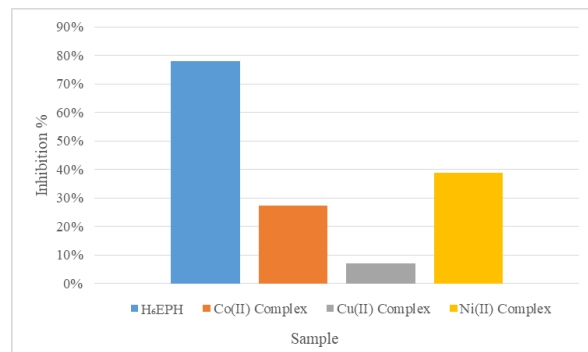


Figure 12. Superoxide dismutase scavenging radicals like activity of H_6EPH and its metal complexes.

H_6EPH and its metal complexes were screened for their superoxide-scavenging activity in the PMS/NADH–NBT system,

and the results are represented in figure 12. In this system, superoxide anion derived from dissolved oxygen by PMS/NADH coupling reaction reduces NBT. The decrease of absorbance at 560 nm with antioxidant activities of the complexes indicates the consumption of superoxide anion in the reaction mixture. There is an apparent variation in the overall scavenging ability among the parent ligand and its metal complexes. The data indicate that H₆EPH had the potent activity of quenching phenazin methosulphate radicals, 69.30 % inhibition while, Ni(II) and

Co(II) complexes exhibit the low Superoxide dismutase like activity with inhibition, 38.80 and 27.20%, respectively. Finally, Cu(II) complex show the lowest antioxidant activity with inhibition of 7.00%.

The high antioxidant capacity of the hydrazone under study can be considered to be an important promising antioxidant. They might help to attenuate the oxidative stress and participate in protection against the harmful action of reactive oxygen species, mainly oxygen free radicals.

4. CONCLUSIONS

A series of divalent Ni (II), Co (II) and Cu (II) complexes of 9S,10S,11R,12R)-9,10-dihydro-9,10-ethanoanthracene-11,12-dicarbonyl)bis(N-phenylhydraziccarboxyamide) (H₆EPH) has been prepared and characterized by conventional techniques. A tetrahedral and octahedral geometry was suggested for the

prepared complexes. Moreover, the ligand and its complexes were screened for DNA binding ability and SOD antioxidant activities. The hydrazone exhibited a potent activity revealing the possibility of utilizing it as an important promising antioxidant.

5. REFERENCES

1. Wang, Y.; Yang, Z. Y.; Wang, B. Synthesis, Characterization and Anti-oxidative Activity of Cobalt(II), Nickel(II) and Iron(II) Schiff Base Complexes. *Trans. Met. Chem.* **2005**, *30*, 879-883, <https://doi.org/10.1007/s11243-005-6166-9>.
2. Maragerum, D.W.; Owens, G.D. *Metal Ions in Biological Systems*, H. Sigel: Marcel Dekker, New York, 1981.
3. Chakraborty, J.; Samanta, B.; Pilet, G., Mitra, S. Synthesis, structure and spectral characterisation of a hydrogen-bonded polymeric manganese(III) Schiff base complex. *J. Struct. Chem.* **2006**, *17*, 585-593, <http://dx.doi.org/10.1007/s11224-006-9076-3>.
4. Rollas, S.; Küçükgüzel, S.G. Biological activities of hydrazone derivatives. *Molecules* **2007**, *12*, 1910-1939, <https://doi.org/10.3390/12081910>.
5. Vicini, P.; Incerti, M.; Doytchinova, I.A.; La Colla, P.; Busonera, B.; Loddo, R. Synthesis and antiproliferative activity of benzo[d]isothiazole hydrazones. *Eur. J. Med. Chem.* **2006**, *41*, 624-632, <https://doi.org/10.1016/j.ejmech.2006.01.010>.
6. Bezerra-Netto, H.J.C.; Lacerda, D.I.; Miranda, A.L.P.; Alves, H.M.; Barreiro, E.J.; Fraga, C.A.M. Design and synthesis of 3,4-methylenedioxy-6-nitrophenoxyacetylhydrazone derivatives obtained from natural safrole: New lead-agents with analgesic and antipyretic properties. *Bioorg. Med. Chem.* **2006**, *14*, 7924-7935, <https://doi.org/10.1016/j.bmc.2006.07.046>.
7. Getautis, V.; Daskeviciene, M.; Malinauskas, T.; Jankauskas, V.; Sidaravicius, J. Influence of the hydroxyl groups on the properties of hydrazone based molecular glasses. *Thin Solid Films* **2008**, *516*, 8979- 8983, <https://doi.org/10.1016/j.tsf.2007.11.074>.
8. Aich, R.; Tran-Van, F.; Goubard, F.; Beouch, L.; Michaleviciute, A.; Grazulevicius, J.V.; Ratier, B.; Chevrot, C. Hydrazone based molecular glasses for solid-state dye-sensitized solar cells. *Thin Solid Films* **2008**, *516*, 7260-7265, <https://doi.org/10.1016/j.tsf.2007.12.125>.
9. Pinto, J.J.; Moreno, C.; Garca-Vargas, M. A very sensitive flow system for the direct determination of copper in natural waters based on spectrophotometric detection. *Talanta* **2004**, *64*, 562-565, <https://doi.org/10.1016/j.talanta.2004.03.009>.
10. Ávila Terra, L.H.S; Guekezian, M.; Gaubeur, I.; Matos, J.R.; Sudrez-Iha, M.E.V. Synthesis, characterization, properties and thermal study of nickel(II)/di-2-pyridyl ketone benzoylhydrazone complex. *Polyhedron* **2002**, *21*, 2375-2380, [https://doi.org/10.1016/S0277-5387\(02\)01185-3](https://doi.org/10.1016/S0277-5387(02)01185-3).
11. Bekheit, M.M.; El-Gammal, O.A.; Tahoon, M.M. Ligational behaviour of biacetylmonoxime- α -naphthoxyacetylhydrazone (H₂BNAH) Towards Some Transition Metal Ions. *Mans. J. Chem.* **2009**, *36*, 129-142.
12. El-Gammal, O.A.; Abu El-Reash, G.M.; Ghazy, S.E.; Radwan, A.H. Synthesis, characterization, molecular modeling and antioxidant activity of (1E, 5E)-1,5- bis(-pyridin-2-yl)ethylidene) carbohydrazide (H₂APC) and its zinc(II), cadmium(II) and mercury (II) complexes. *J. Mol. Struct.* **2012**, *1020*, 6-15, <http://dx.doi.org/10.1016%2Fj.molstruc.2012.04.029>.
13. El-Gammal, O.A.; Rakha, T.H.; Metwally, H.M.; Abu El-Reash, G.M. Synthesis, characterization, DFT and biological studies of isatin picolinohydrazone and its Zn(II), Cd(II) and Hg(II) complexes *Spectrochimica Acta Part A* **2014**, *127*, 144-156, <https://doi.org/10.1016/j.saa.2014.02.008>.
14. El-Gammal, O.A.; Abd Al-Gader, I.M.; El-Asmy, A.A. Synthesis, characterization, biological activity of binuclear Co(II), Cu(II) and mononuclear Ni(II) complexes of bulky multi-dentate thiosemicarbazide. *Spectrochimica Acta Part A* **2014**, *128*, 759-772, <https://doi.org/10.1016/j.saa.2014.01.119>.
15. Delley, B. Hardness conserving semilocal pseudopotentials. *Phys. Rev. B Condens. Matter* **2002**, *66*, 155125-155129, <https://doi.org/10.1103/PhysRevB.66.155125>.
16. *Modeling and Simulation Solutions for Chemicals and Materials Research*. Materials Studio, Version 7.0, Accelrys software Inc., San Diego, USA, **2011**.
17. Hehre, W.J. *Ab initio molecular orbital theory*, Wiley-Interscience, 1986.
18. Kessi, A.; Delley, B. Density functional crystal vs. cluster models as applied to zeolites. *Int. J. Quantum Chem.* **1998**, *68*, 135-144, [https://doi.org/10.1002/\(SICI\)1097-461X\(1998\)68:2<135::AID-QUA6>3.0.CO;2-W](https://doi.org/10.1002/(SICI)1097-461X(1998)68:2<135::AID-QUA6>3.0.CO;2-W).
19. Hammer, B.; Hansen, L.B.; Nørskov, J.K. Improved adsorption energetics within density-functional theory using revised Perdew-Burke-Ernzerhof functionals. *Phys. Rev. B: Condens. Matter* **1999**, *59*, 7413-7421, <https://doi.org/10.1103/PhysRevB.59.7413>.
20. Ghaly, M.A.; El-Bendary, E.R.; Shehata, I.A.; Bayomi, S.M.; Habib, S. Synthesis, Antimicrobial Activity, DNA-Binding Affinity and Molecular Docking of Certain 1,2,4- Triazolo[1,5-a]Pyrimidines as Nalidixic Acid Isosteres *J. Am. Sci.* **2012**, *8*, 617-628.

21. Krishna, P.M.; Reddy, K.H.; Pandey, J.P.; Siddavattam, D. Synthesis, characterization, DNA binding and nuclease activity of binuclear copper(II) complexes of cuminaldehyde thiosemicarbazones. *Transition Met. Chem.* **2008**, *33*, 661-668, <https://doi.org/10.1007/s11243-008-9094-7>.
22. Dhar, S.; Reddy, P.A.N.; Nethaji, Mahadevan, M. S.; Saha, M. K.; Chakravarty, A. R. Effect of steric encumbrance of tris(3-phenylpyrazolyl)borate on the structure and properties of ternary copper(II) complexes having N,N-donor heterocyclic bases. *Inorg. Chem.* **2002**, *41*, 3469-3476.
23. Geary; W.J. The Use of Conductivity Measurements in Organic Solvents for the Characterisation of Coordination Compounds. *Coord. Chem. Rev.* **1971**, *7*, 81-122, <https://doi.org/10.1021/ic0201396>.
24. El-Gammal, O.A.; El-Asmy, A.A. Synthesis and Spectral Characterization of 1-(aminoformyl-n-phenylform)-4-ethyl Thiosemicarbazide and its Metal Complexes. *J. Coord. Chem.* **2008**, *61*, 2296-2306, <http://dx.doi.org/10.1080/00958970801907748>.
25. El-Gammal, O.A.; Abu El-Reash, G.M.; Ahmed, S.F. Structural, spectral, thermal and biological studies on 2-oxo-N-O-((4-oxo-4H-chromen-3-yl)methylene)-2-(phenylamino) acetohydrazide (H_2L) and its metal complexes. *J. Mol. Struct.* **2012**, *1007*, 1-10, <https://doi.org/10.1016/j.molstruc.2011.03.043>.
26. El-Gammal, O.A.; Abu El-Reash, G.M.; Ghazy, S.E.; Radwan, A.H. Synthesis, characterization, molecular modeling and antioxidant activity of (1E, 5E)-1,5-bis(-pyridin-2-yl)ethylidene) carbohydrazide (H_2APC) and its zinc(II) , cadmium(II) and mercury (II) complexes. *J. Mol. Struct.* **2012**, *1020*, 6-15, <http://dx.doi.org/10.1016/j.molstruc.2012.04.029>.
27. El-Gammal, O.A.; Saad, D.A.; El-Asmy, A.A. Synthesis of Copper complexes of a new symmetrical dihydrazone: Characterization, XRD studies, DFT calculations and biological activity. *Der PharmaChemica* **2016**, *8*, 317-327.
28. El-Gammal, O.A.; Bekheit, M.M.; Tahooon, M. Synthesis, characterization and biological activity of 2-acetylpyridine- α -naphthoxyacetylhydrazone its metal complexes. *Spectrochimica Acta Part A* **2015**, *135*, 597-607, <https://doi.org/10.1016/j.saa.2014.05.071>.
29. El-Gammal, O.A.; Bekheit, M.M.; El-Brashy, S.A. Synthesis, characterization and in vitro antimicrobial studies of Co (II), Ni (II) and Cu (II) complexes derived from macrocyclic compartmental ligand. *Spectrochimica Acta Part A* **2015**, *137*, 207-219, <https://doi.org/10.1016/j.saa.2014.08.016>.
30. El-Gammal, O.A.; Abu El-Reash, G.M.; Youssef, T.A.; Mefreh, M. Synthesis, spectral characterization, computational calculations and biological activity of complexes designed from NNO donor Schiff-base ligand. *Spectrochimica Acta Part A* **2015**, *146*, 163-176, <https://doi.org/10.1016/j.saa.2015.01.043>.
31. El-Gammal, O. A.; El-Morsy, F.E.; Jeragh, B.; El-Asmy, A.A. Chelation Behavior of bis (1-(Pyridin-2-yl) ethylidene)-malonohydrazide towards Some Transition Metal Ions. *Canad. Chem. Trans.* **2013**, *1*, 277-291.
32. El-Gammal,O.A.; Abu El-Reash, G.M.; Ghazy, S.E.; Yousef, T.A. Heterocyclic substituted thiosemicarbazides and their Cu (II) complexes: synthesis, spectral characterization, thermal, molecular modeling, and DNA degradation studies. *J. Coord. Chem.* **2012**, *10*, 1655-1671, <https://doi.org/10.1080/00958972.2012.674519>.
33. Neuhaus, A. Über die Gastkomponenten der Mischkristalle vom Typus des Eisensalmiaks *Z. Kristallogr- Cryst. Mater.* **1938**, *98*, 112-142.
34. Coats, A.; Redfern, J. Kinetic Parameters from Thermogravimetric Data. *Nature* **1964**, *201*, 68-69, <https://doi.org/10.1038/pol.1965.110031106>.
35. Horowitz, H.H.; Metzger, G.A New Analysis of Thermogravimetric Traces. *Anal. Chem.* **1963**, *35*, 1464-1468, <https://doi.org/10.1021/ac60203a013>.
36. Kenawy, I.; Hafez, M.; Lashein, R. Thermal Decomposition of Chloromethylated Poly(styrene)-PAN Resin and Its Complexes with Some Transition Metal Ions. *J. Therm. Anal. Calorim.* **2001**, *65*, 723-736, <https://doi.org/10.1023/A:1011999325998>.
37. Siddalingaiah, A.H.M; Naik, S.G. Spectroscopic and thermogravimetric studies on Ni(II), Cu(II) and Zn(II) complexes of di (2, 6-dichlorophenyl) carbazole. *J. Mol. Struct.: Theochem* **2002**, *582*, 129-136, [https://doi.org/10.1016/S0166-1280\(01\)00777-1](https://doi.org/10.1016/S0166-1280(01)00777-1).
38. Kandil, S.S.; El-Hefnawy, G.B.; Baker, E.A. Thermal and spectral studies of 5-(phenylazo)-2-thiohydantoin and 5-(2-hydroxyphenylazo)-2-thiohydantoin complexes of cobalt(II), nickel(II) and copper(II). *Thermochim. Acta* **2004**, *414*, 105-113, <https://doi.org/10.1016/j.tca.2003.11.021>.
39. El-Gammal, O.A. Synthesis, characterization, molecular modeling and antimicrobial activity of 2-(2-(ethylcarbamothioyl)hydrazinyl)-2-oxo-N-phenylacetamide copper complexes. *Spectrochim. Acta part A* **2010**, *75*, 533-542, <https://doi.org/10.1016/j.saa.2009.11.007>.
40. El-Gammal, O.A.; Al-Hossainy, A.F.; El-Brashy, S.A. Spectroscopic, DFT, optical band gap, powder X-ray diffraction and bleomycin-dependant DNA studies of Co(II), Ni(II) and Cu(II) complexes derived from macrocyclic Schiff base. *J. Mol. Struct.* **2018**, *1165*, 177-195, <https://doi.org/10.1016/j.molstruc.2018.03.057>.
41. Raman, N.; Muthuraj, V.; Ravichandran, S.; Kulandaivasamy, A. Synthesis, characterisation and electrochemical behaviour of Cu(II), Co(II), Ni(II) and Zn(II) complexes derived from acetylacetone andp-anisidine and their antimicrobial activity. *Proc. Ind. Acad. Sci.* **2003**, *115*, 161-167, <https://doi.org/10.1007/BF02704255>.
42. El-Gammal, O.A. Mononuclear and binuclear complexes derived from hydrazone Schiff base NON donor ligand: Synthesis, structure, theoretical and biological studies. *Inorgan. Chim. Acta* **2015**, *435*, 73-81, <https://doi.org/10.1016/j.ica.2015.06.009>.
43. Ramadan, A.M. Macroyclic nickel(II) complexes: Synthesis, characterization, superoxide scavenging activity and DNA-binding. *J. Mol. Struct.* **2012**, *1015*, 56-66, <https://doi.org/10.1016/j.molstruc.2012.01.048>.



Table 1S. Selected bond lengths (\AA) of H_6EPH ligand.

Bond	Length (\AA)	Bond	Length (\AA)	Bond	Length (\AA)
C(10)-C(11)	1.401	C(15)-C(16)	1.538	C(16)-N(17)	1.359
C(4)-C(5)	1.409	C(20)-N(21)	1.410	C(19)-C(20)	1.532
C(8)-C(9)	1.397	C(5)-C(6)	1.399	C(3)-C(4)	1.404
C(2)-C(3)	1.406	C(6)-C(1)	1.406	C(1)-C(2)	1.400
C(9)-C(10)	1.408	C(41)-C(42)	1.401	C(40)-C(41)	1.402
C(39)-C(40)	1.404	C(38)-C(39)	1.403	C(42)-C(37)	1.415
C(37)-C(38)	1.409	N(36)-C(37)	1.416	C(34)-N(36)	1.391
C(34)-O(35)	1.227	C(32)-C(33)	1.402	C(31)-C(32)	1.399
C(30)-C(31)	1.400	C(29)-C(30)	1.399	C(33)-C(28)	1.408
C(28)-C(29)	1.406	N(27)-C(28)	1.423	C(25)-N(27)	1.394
C(25)-O(26)	1.244	N(22)-C(34)	1.410	N(21)-N(22)	1.382
C(20)-O(23)	1.230	N(18)-C(25)	1.385	N(17)-N(18)	1.392
C(16)-O(24)	1.252	C(15)-C(19)	1.579	C(14)-C(19)	1.595
C(13)-C(15)	1.587	C(11)-C(12)	1.406	C(13)-C(8)	1.525
C(7)-C(14)	1.521	C(12)-C(7)	1.399	C(7)-C(8)	1.410
C(14)-C(5)	1.528	C(4)-C(13)	1.524		

Table 2S. Selected bond angles ($^{\circ}$) of H_6EPH ligand.

Angle	Degree ($^{\circ}$)	Angle	Degree ($^{\circ}$)	Angle	Degree ($^{\circ}$)
C(19)-C(15)-C(16)	113.00	N(17)-C(16)-C(15)	117.29	N(21)-C(20)-C(19)	112.02
C(5)-C(6)-C(1)	119.13	C(6)-C(5)-C(4)	120.59	C(5)-C(4)-C(3)	120.19
C(4)-C(3)-C(2)	119.14	C(3)-C(2)-C(1)	120.48	C(6)-C(1)-C(2)	120.46
C(41)-C(42)-C(37)	120.46	C(42)-C(41)-C(40)	120.12	C(41)-C(40)-C(39)	119.44
C(40)-C(39)-C(38)	121.04	C(39)-C(38)-C(37)	119.54	C(42)-C(37)-C(38)	119.39
C(42)-C(37)-N(36)	116.84	C(38)-C(37)-N(36)	123.75	C(37)-N(36)-C(34)	129.08
N(36)-C(34)-O(35)	126.70	N(36)-C(34)-N(22)	113.83	O(35)-C(34)-N(22)	119.48
C(32)-C(33)-C(28)	120.10	C(33)-C(32)-C(31)	120.87	C(32)-C(31)-C(30)	118.79
C(31)-C(30)-C(29)	121.02	C(30)-C(29)-C(28)	120.08	C(33)-C(28)-C(29)	119.09
C(33)-C(28)-N(27)	118.02	C(29)-C(28)-N(27)	122.78	C(28)-N(27)-C(25)	125.44
N(27)-C(25)-O(26)	124.83	N(27)-C(25)-N(18)	114.36	O(26)-C(25)-N(18)	120.78
C(34)-N(22)-N(21)	122.53	N(22)-N(21)-C(20)	122.66	O(23)-C(20)-N(21)	121.29
O(23)-C(20)-C(19)	125.86	C(20)-C(19)-C(15)	117.29	C(20)-C(19)-C(14)	108.61
C(15)-C(19)-C(14)	107.92	C(25)-N(18)-N(17)	115.59	N(18)-N(17)-C(16)	119.56
O(24)-C(16)-N(17)	122.73	O(24)-C(16)-C(15)	119.89	C(19)-C(15)-C(13)	109.40
C(16)-C(15)-C(13)	117.88	C(19)-C(14)-C(7)	105.64	C(19)-C(14)-C(5)	110.85
C(7)-C(14)-C(5)	105.94	C(15)-C(13)-C(8)	105.75	C(15)-C(13)-C(4)	110.93
C(8)-C(13)-C(4)	105.02	C(11)-C(12)-C(7)	119.28	C(12)-C(11)-C(10)	120.07
C(11)-C(10)-C(9)	120.59	C(10)-C(9)-C(8)	119.41	C(13)-C(8)-C(9)	126.58
C(13)-C(8)-C(7)	113.42	C(9)-C(8)-C(7)	119.98	C(14)-C(7)-C(12)	126.86
C(14)-C(7)-C(8)	112.46	C(12)-C(7)-C(8)	120.67	C(14)-C(5)-C(6)	126.11
C(14)-C(5)-C(4)	113.26	C(13)-C(4)-C(5)	112.56	C(13)-C(4)-C(3)	127.26

Table 3S. Selected bond lengths (\AA) of $[\text{Co}_2(\text{H}_4\text{EPH})(\text{OH})_2(\text{H}_2\text{O})_4].5\text{H}_2\text{O}$ complex.

Bond	Length (\AA)	Bond	Length (\AA)	Bond	Length (\AA)
C(10)-C(11)	1.403	C(15)-C(16)	1.545	C(16)-N(17)	1.327
C(4)-C(5)	1.411	C(20)-N(21)	1.333	C(19)-C(20)	1.531
C(8)-C(9)	1.4	C(5)-C(6)	1.4	C(3)-C(4)	1.402
C(2)-C(3)	1.409	C(6)-C(1)	1.408	C(1)-C(2)	1.402
C(9)-C(10)	1.406	C(27)-C(28)	1.406	N(26)-C(27)	1.423
O(48)-Co(44)	1.908	O(46)-Co(44)	2.064	O(47)-Co(43)	1.877
O(45)-Co(43)	2.092	Co(44)-Co(43)	2.605	O(42)-Co(43)	2.228
C(40)-C(41)	1.397	C(39)-C(40)	1.404	C(38)-C(39)	1.402
C(37)-C(38)	1.404	C(41)-C(36)	1.413	C(36)-C(37)	1.406
N(35)-C(36)	1.422	O(34)-Co(44)	2.495	C(33)-N(35)	1.363
C(33)-O(34)	1.248	C(31)-C(32)	1.396	C(30)-C(31)	1.403
C(29)-C(30)	1.403	C(28)-C(29)	1.406	C(32)-C(27)	1.414
C(25)-O(42)	1.268	C(25)-N(26)	1.36	O(24)-Co(43)	1.889
O(23)-Co(44)	1.93	N(22)-Co(44)	2.072	N(22)-C(33)	1.467
N(21)-N(22)	1.51	C(20)-O(23)	1.293	N(18)-Co(43)	2.157
N(18)-C(25)	1.454	N(17)-N(18)	1.539	C(16)-O(24)	1.32
C(15)-C(19)	1.619	C(14)-C(19)	1.582	C(13)-C(15)	1.577
C(11)-C(12)	1.405	C(13)-C(8)	1.524	C(7)-C(14)	1.523
C(12)-C(7)	1.4	C(7)-C(8)	1.407	C(14)-C(5)	1.523
C(4)-C(13)	1.529				

Table 4S. Selected bond angles ($^{\circ}$) of $[\text{Co}_2(\text{H}_4\text{EPH})(\text{OH})_2(\text{H}_2\text{O})_4]\cdot 5\text{H}_2\text{O}$ complex.

Angle	Degree ($^{\circ}$)	Angle	Degree ($^{\circ}$)	Angle	Degree ($^{\circ}$)
C(19)-C(15)-C(16)	114.574	N(17)-C(16)-C(15)	122.895	N(21)-C(20)-C(19)	115.903
C(5)-C(6)-C(1)	119.245	C(6)-C(5)-C(4)	120.577	C(5)-C(4)-C(3)	120.032
C(4)-C(3)-C(2)	119.443	C(3)-C(2)-C(1)	120.351	C(6)-C(1)-C(2)	120.35
C(28)-C(27)-N(26)	125.902	O(48)-Co(44)-O(46)	87.788	O(48)-Co(44)-Co(43)	89.943
O(48)-Co(44)-O(34)	104.438	O(48)-Co(44)-O(23)	94.156	O(48)-Co(44)-N(22)	163.461
O(46)-Co(44)-Co(43)	98.932	O(46)-Co(44)-O(34)	90.45	O(46)-Co(44)-O(23)	177.119
O(46)-Co(44)-N(22)	98.083	Co(43)-Co(44)-O(34)	163.171	Co(43)-Co(44)-O(23)	83.211
Co(43)-Co(44)-N(22)	104.284	O(34)-Co(44)-O(23)	87.008	O(34)-Co(44)-N(22)	60.292
O(23)-Co(44)-N(22)	79.476	O(47)-Co(43)-O(45)	170.674	O(47)-Co(43)-Co(44)	84.481
O(47)-Co(43)-O(42)	76.78	O(47)-Co(43)-O(24)	98.379	O(47)-Co(43)-N(18)	80.971
O(45)-Co(43)-Co(44)	96.521	O(45)-Co(43)-O(42)	95.139	O(45)-Co(43)-O(24)	90.861
O(45)-Co(43)-N(18)	99.728	Co(44)-Co(43)-O(42)	124.158	Co(44)-Co(43)-O(24)	91.966
Co(44)-Co(43)-N(18)	161.351	O(42)-Co(43)-O(24)	142.199	O(42)-Co(43)-N(18)	63.446
O(24)-Co(43)-N(18)	78.753	Co(43)-O(42)-C(25)	88.735	C(40)-C(41)-C(36)	120.198
C(41)-C(40)-C(39)	120.652	C(40)-C(39)-C(38)	118.977	C(39)-C(38)-C(37)	121.034
C(38)-C(37)-C(36)	119.727	C(41)-C(36)-C(37)	119.38	C(41)-C(36)-N(35)	115.593
C(37)-C(36)-N(35)	124.995	C(36)-N(35)-C(33)	135.591	Co(44)-O(34)-C(33)	84.334
N(35)-C(33)-O(34)	120.376	N(35)-C(33)-N(22)	122.22	O(34)-C(33)-N(22)	117.383
C(31)-C(32)-C(27)	120.568	C(32)-C(31)-C(30)	119.762	C(31)-C(30)-C(29)	119.59
C(30)-C(29)-C(28)	121.366	C(29)-C(28)-C(27)	118.679	C(32)-C(27)-C(28)	120.033
C(32)-C(27)-N(26)	114.062	C(27)-N(26)-C(25)	137.608	O(42)-C(25)-N(26)	117.244
O(42)-C(25)-N(18)	115.665	N(26)-C(25)-N(18)	126.013	Co(43)-O(24)-C(16)	103.632
Co(44)-O(23)-C(20)	112.139	Co(44)-N(22)-C(33)	96.802	Co(44)-N(22)-N(21)	109.909
C(33)-N(22)-N(21)	111.013	N(22)-N(21)-C(20)	106.818	O(23)-C(20)-N(21)	125.433
O(23)-C(20)-C(19)	118.637	C(20)-C(19)-C(15)	117.316	C(20)-C(19)-C(14)	111.274
C(15)-C(19)-C(14)	108.432	Co(43)-N(18)-C(25)	87.085	Co(43)-N(18)-N(17)	99.101
C(25)-N(18)-N(17)	127.73	N(18)-N(17)-C(16)	106.527	O(24)-C(16)-N(17)	125.987
O(24)-C(16)-C(15)	111.011	C(19)-C(15)-C(13)	107.984	C(16)-C(15)-C(13)	115.783
C(19)-C(14)-C(7)	109.742	C(19)-C(14)-C(5)	105.494	C(7)-C(14)-C(5)	106.795
C(15)-C(13)-C(8)	108.103	C(15)-C(13)-C(4)	107.063	C(8)-C(13)-C(4)	106.726
C(11)-C(12)-C(7)	119.084	C(12)-C(11)-C(10)	120.369	C(11)-C(10)-C(9)	120.514
C(10)-C(9)-C(8)	119.08	C(13)-C(8)-C(9)	126.177	C(13)-C(8)-C(7)	113.424
C(9)-C(8)-C(7)	120.398	C(14)-C(7)-C(12)	126.434	C(14)-C(7)-C(8)	113.005
C(12)-C(7)-C(8)	120.55	C(14)-C(5)-C(6)	126.457	C(14)-C(5)-C(4)	112.962
C(13)-C(4)-C(5)	113.199	C(13)-C(4)-C(3)	126.757		

Table 5S. Selected bond lengths (\AA) of $[\text{Ni}_2(\text{H}_4\text{EPH})(\text{OH})_2(\text{H}_2\text{O})_2]\cdot 4\text{H}_2\text{O}$ complex.

Bond	Length	Bond	Length	Bond	Length
O(48)-H(80)	0.975	C(30)-C(31)	1.402	C(15)-C(16)	1.527
O(48)-H(79)	0.994	C(29)-H(65)	1.091	C(14)-H(58)	1.096
O(47)-H(78)	1.009	C(29)-C(30)	1.403	C(14)-C(19)	1.578
O(47)-H(77)	0.975	C(28)-H(64)	1.085	C(13)-H(57)	1.098
O(46)-H(76)	0.974	C(28)-C(29)	1.401	C(13)-C(15)	1.583
O(45)-H(75)	0.974	C(32)-C(27)	1.409	C(12)-H(56)	1.093
O(47)-Ni(44)	1.968	C(27)-C(28)	1.408	C(11)-H(55)	1.092
O(46)-Ni(44)	1.868	N(26)-H(63)	1.017	C(11)-C(12)	1.407
O(48)-Ni(43)	1.981	N(26)-C(27)	1.419	C(10)-H(54)	1.091
O(45)-Ni(43)	1.851	C(25)-O(42)	1.225	C(10)-C(11)	1.405
C(41)-H(74)	1.093	C(25)-N(26)	1.363	C(9)-H(53)	1.093
C(40)-H(73)	1.09	O(24)-Ni(43)	1.876	C(9)-C(10)	1.404
C(40)-C(41)	1.4	O(23)-Ni(44)	1.88	C(13)-C(8)	1.518
C(39)-H(72)	1.092	N(22)-H(62)	1.026	C(8)-C(9)	1.398
C(39)-C(40)	1.403	N(22)-Ni(44)	1.93	C(7)-C(14)	1.527
C(38)-H(71)	1.093	N(22)-C(33)	1.485	C(12)-C(7)	1.398
C(38)-C(39)	1.402	N(21)-N(22)	1.5	C(7)-C(8)	1.413
C(37)-H(70)	1.09	C(20)-O(23)	1.313	C(6)-H(52)	1.092
C(37)-C(38)	1.402	C(20)-N(21)	1.318	C(14)-C(5)	1.522
C(41)-C(36)	1.409	C(19)-H(61)	1.099	C(5)-C(6)	1.398
C(36)-C(37)	1.408	C(19)-C(20)	1.527	C(13)-C(4)	1.52
N(35)-H(69)	1.018	N(18)-H(60)	1.028	C(4)-C(5)	1.414
N(35)-C(36)	1.427	N(18)-Ni(43)	1.914	C(3)-H(51)	1.093
C(33)-N(35)	1.377	N(18)-C(25)	1.501	C(3)-C(4)	1.399
C(33)-O(34)	1.227	N(17)-N(18)	1.492	C(2)-H(50)	1.093
C(32)-H(68)	1.091	C(16)-O(24)	1.316	C(2)-C(3)	1.406
C(31)-H(67)	1.091	C(16)-N(17)	1.318	C(1)-H(49)	1.093

C(31)-C(32)	1.399	C(15)-H(59)	1.096	C(6)-C(1)	1.405
C(30)-H(66)	1.091	C(15)-C(19)	1.568	C(1)-C(2)	1.405
Table 6S. Selected bond angles ($^{\circ}$) of $[\text{Ni}_2(\text{H}_4\text{EPH})(\text{OH})_2(\text{H}_2\text{O})_2] \cdot 4\text{H}_2\text{O}$ complex.					
Angle	Degree	Angle	Degree		
H(80)-O(48)-H(79)	108.38	C(33)-N(22)-N(21)	109.96		
H(80)-O(48)-Ni(43)	110.927	N(22)-N(21)-C(20)	107.135		
H(79)-O(48)-Ni(43)	86.182	O(23)-C(20)-N(21)	125.253		
H(78)-O(47)-H(77)	107.993	O(23)-C(20)-C(19)	116.194		
H(78)-O(47)-Ni(44)	84.014	N(21)-C(20)-C(19)	118.549		
H(77)-O(47)-Ni(44)	111.971	H(61)-C(19)-C(20)	106.142		
H(76)-O(46)-Ni(44)	109.074	H(61)-C(19)-C(15)	107.702		
H(75)-O(45)-Ni(43)	109.449	H(61)-C(19)-C(14)	106.654		
O(47)-Ni(44)-O(46)	80.09	C(20)-C(19)-C(15)	111.486		
O(47)-Ni(44)-O(23)	96.115	C(20)-C(19)-C(14)	115.298		
O(47)-Ni(44)-N(22)	178.748	C(15)-C(19)-C(14)	109.147		
O(46)-Ni(44)-O(23)	174.297	H(60)-N(18)-Ni(43)	107.575		
O(46)-Ni(44)-N(22)	100.099	H(60)-N(18)-C(25)	101.725		
O(23)-Ni(44)-N(22)	83.789	H(60)-N(18)-N(17)	106.767		
O(48)-Ni(43)-O(45)	80.555	Ni(43)-N(18)-C(25)	118.564		
O(48)-Ni(43)-O(24)	95.21	Ni(43)-N(18)-N(17)	111.408		
O(48)-Ni(43)-N(18)	179.971	C(25)-N(18)-N(17)	109.731		
O(45)-Ni(43)-O(24)	170.583	N(18)-N(17)-C(16)	107.831		
O(45)-Ni(43)-N(18)	99.454	O(24)-C(16)-N(17)	125.113		
O(24)-Ni(43)-N(18)	84.785	O(24)-C(16)-C(15)	119.094		
H(74)-C(41)-C(40)	120.536	N(17)-C(16)-C(15)	115.792		
H(74)-C(41)-C(36)	119.692	H(59)-C(15)-C(19)	110.058		
C(40)-C(41)-C(36)	119.767	H(59)-C(15)-C(16)	105.527		
H(73)-C(40)-C(41)	119.385	H(59)-C(15)-C(13)	106.264		
H(73)-C(40)-C(39)	120.262	C(19)-C(15)-C(16)	112.991		
C(41)-C(40)-C(39)	120.349	C(19)-C(15)-C(13)	109.026		
H(72)-C(39)-C(40)	120.317	C(16)-C(15)-C(13)	112.699		
H(72)-C(39)-C(38)	120.003	H(58)-C(14)-C(19)	110.433		
C(40)-C(39)-C(38)	119.675	H(58)-C(14)-C(7)	112.391		
H(71)-C(38)-C(39)	120.277	H(58)-C(14)-C(5)	113.006		
H(71)-C(38)-C(37)	119.113	C(19)-C(14)-C(7)	105.496		
C(39)-C(38)-C(37)	120.595	C(19)-C(14)-C(5)	107.339		
H(70)-C(37)-C(38)	120.549	C(7)-C(14)-C(5)	107.772		
H(70)-C(37)-C(36)	120.017	H(57)-C(13)-C(15)	109.882		
C(38)-C(37)-C(36)	119.433	H(57)-C(13)-C(8)	113.398		
C(41)-C(36)-C(37)	120.168	H(57)-C(13)-C(4)	112.184		
C(41)-C(36)-N(35)	118.426	C(15)-C(13)-C(8)	108.907		
C(37)-C(36)-N(35)	121.387	C(15)-C(13)-C(4)	104.281		
H(69)-N(35)-C(36)	117.051	C(8)-C(13)-C(4)	107.745		
H(69)-N(35)-C(33)	111.624	H(56)-C(12)-C(11)	119.989		
C(36)-N(35)-C(33)	130.964	H(56)-C(12)-C(7)	120.369		
N(35)-C(33)-O(34)	122.865	C(11)-C(12)-C(7)	119.638		
N(35)-C(33)-N(22)	115.475	H(55)-C(11)-C(12)	119.263		
O(34)-C(33)-N(22)	121.648	H(55)-C(11)-C(10)	120.108		
H(68)-C(32)-C(31)	119.718	C(12)-C(11)-C(10)	120.629		
H(68)-C(32)-C(27)	119.883	H(54)-C(10)-C(11)	120.302		
C(31)-C(32)-C(27)	120.392	H(54)-C(10)-C(9)	119.904		
H(67)-C(31)-C(32)	119.037	C(11)-C(10)-C(9)	119.792		
H(67)-C(31)-C(30)	120.447	H(53)-C(9)-C(10)	120.47		
C(32)-C(31)-C(30)	120.514	H(53)-C(9)-C(8)	119.956		
H(66)-C(30)-C(31)	120.663	C(10)-C(9)-C(8)	119.573		
H(66)-C(30)-C(29)	120.5	C(13)-C(8)-C(9)	125.94		
C(31)-C(30)-C(29)	118.828	C(13)-C(8)-C(7)	113.27		
H(65)-C(29)-C(30)	119.961	C(9)-C(8)-C(7)	120.782		
H(65)-C(29)-C(28)	118.693	C(14)-C(7)-C(12)	127.404		
C(30)-C(29)-C(28)	121.345	C(14)-C(7)-C(8)	113.012		
H(64)-C(28)-C(29)	120.619	C(12)-C(7)-C(8)	119.576		
H(64)-C(28)-C(27)	119.885	H(52)-C(6)-C(5)	119.77		
C(29)-C(28)-C(27)	119.493	H(52)-C(6)-C(1)	120.621		
C(32)-C(27)-C(28)	119.418	C(5)-C(6)-C(1)	119.609		
C(32)-C(27)-N(26)	116.928	C(14)-C(5)-C(6)	126.678		
C(28)-C(27)-N(26)	123.649	C(14)-C(5)-C(4)	113.28		
H(63)-N(26)-C(27)	115.776	C(6)-C(5)-C(4)	120.042		
H(63)-N(26)-C(25)	115.44	C(13)-C(4)-C(5)	112.997		

Angle	Degree	Angle	Degree
C(27)-N(26)-C(25)	128.655	C(13)-C(4)-C(3)	126.552
O(42)-C(25)-N(26)	129.503	C(5)-C(4)-C(3)	120.398
O(42)-C(25)-N(18)	118.837	H(51)-C(3)-C(4)	120.433
N(26)-C(25)-N(18)	111.628	H(51)-C(3)-C(2)	120.169
Ni(43)-O(24)-C(16)	110.825	C(4)-C(3)-C(2)	119.395
Ni(44)-O(23)-C(20)	110.428	H(50)-C(2)-C(3)	119.913
H(62)-N(22)-Ni(44)	114.226	H(50)-C(2)-C(1)	119.818
H(62)-N(22)-C(33)	109.524	C(3)-C(2)-C(1)	120.264
H(62)-N(22)-N(21)	105.431	H(49)-C(1)-C(6)	119.928
Ni(44)-N(22)-C(33)	107.36	H(49)-C(1)-C(2)	119.786
Ni(44)-N(22)-N(21)	110.324	C(6)-C(1)-C(2)	120.285

 Table 7S. Selected bond lengths (Å) of [Cu₂(H₆EPH)(Cl)₄]·4H₂O complex.

Bond	Length	Bond	Length	Bond	Length
Cl(48)-Cu(44)	2.154	C(32)-C(27)	1.408	C(14)-C(19)	1.601
Cl(47)-Cu(44)	2.216	C(27)-C(28)	1.404	C(13)-H(57)	1.093
Cl(46)-Cu(43)	2.157	N(26)-H(65)	1.018	C(13)-C(15)	1.591
Cl(45)-Cu(43)	2.195	N(26)-C(27)	1.433	C(12)-H(56)	1.092
C(41)-H(76)	1.093	C(25)-O(42)	1.233	C(11)-H(55)	1.09
C(40)-H(75)	1.09	C(25)-N(26)	1.385	C(11)-C(12)	1.405
C(40)-C(41)	1.396	O(24)-Cu(43)	2.077	C(10)-H(54)	1.09
C(39)-H(74)	1.09	O(23)-Cu(44)	2.195	C(10)-C(11)	1.399
C(39)-C(40)	1.405	N(22)-H(64)	1.028	C(9)-H(53)	1.089
C(38)-H(73)	1.092	N(22)-Cu(44)	2.881	C(9)-C(10)	1.403
C(38)-C(39)	1.402	N(22)-C(33)	1.403	C(13)-C(8)	1.511
C(37)-H(72)	1.085	N(21)-H(63)	1.022	C(8)-C(9)	1.397
C(37)-C(38)	1.398	N(21)-N(22)	1.388	C(7)-C(14)	1.505
C(41)-C(36)	1.413	C(20)-O(23)	1.258	C(12)-C(7)	1.4
C(36)-C(37)	1.411	C(20)-N(21)	1.369	C(7)-C(8)	1.413
N(35)-H(71)	1.024	C(19)-H(62)	1.102	C(6)-H(52)	1.094
N(35)-C(36)	1.412	C(19)-C(20)	1.518	C(14)-C(5)	1.623
C(33)-N(35)	1.388	N(18)-H(61)	1.024	C(5)-C(6)	1.491
C(33)-O(34)	1.237	N(18)-Cu(43)	2.926	C(13)-C(4)	1.605
C(32)-H(70)	1.092	N(18)-C(25)	1.422	C(4)-C(5)	1.56
C(31)-H(69)	1.091	N(17)-H(60)	1.019	C(3)-H(51)	1.09
C(31)-C(32)	1.399	N(17)-N(18)	1.398	C(3)-C(4)	1.497
C(30)-H(68)	1.092	C(16)-O(24)	1.253	C(2)-H(50)	1.091
C(30)-C(31)	1.401	C(16)-N(17)	1.366	C(2)-C(3)	1.359
C(29)-H(67)	1.091	C(15)-H(59)	1.1	C(1)-H(49)	1.09
C(29)-C(30)	1.402	C(15)-C(19)	3.319	C(6)-C(1)	1.362
C(28)-H(66)	1.089	C(15)-C(16)	1.521	C(1)-C(2)	1.469
C(28)-C(29)	1.402	C(14)-H(58)	1.097		

 Table 8S. Selected bond angles (°) of [Cu₂(H₆EPH)(Cl)₄]·4H₂O complex.

Angle	Degree	Angle	Degree
Cl(48)-Cu(44)-Cl(47)	135.676	N(21)-C(20)-C(19)	116.404
Cl(48)-Cu(44)-O(23)	119.041	H(62)-C(19)-C(20)	108.829
Cl(48)-Cu(44)-N(22)	125.037	H(62)-C(19)-C(15)	121.374
Cl(47)-Cu(44)-O(23)	105.28	H(62)-C(19)-C(14)	109.044
Cl(47)-Cu(44)-N(22)	75.065	C(20)-C(19)-C(15)	128.163
O(23)-Cu(44)-N(22)	62.536	C(20)-C(19)-C(14)	122.75
Cl(46)-Cu(43)-Cl(45)	154.233	C(15)-C(19)-C(14)	52.624
Cl(46)-Cu(43)-O(24)	103.253	H(61)-N(18)-Cu(43)	77.427
Cl(46)-Cu(43)-N(18)	109.408	H(61)-N(18)-C(25)	110.258
Cl(45)-Cu(43)-O(24)	102.395	H(61)-N(18)-N(17)	113.785
Cl(45)-Cu(43)-N(18)	83.736	Cu(43)-N(18)-C(25)	127.467
O(24)-Cu(43)-N(18)	65.155	Cu(43)-N(18)-N(17)	97.125
H(76)-C(41)-C(40)	119.975	C(25)-N(18)-N(17)	122.519
H(76)-C(41)-C(36)	119.599	H(60)-N(17)-N(18)	118.59
C(40)-C(41)-C(36)	120.424	H(60)-N(17)-C(16)	119.417
H(75)-C(40)-C(41)	119.598	N(18)-N(17)-C(16)	121.663
H(75)-C(40)-C(39)	120.496	O(24)-C(16)-N(17)	123.062
C(41)-C(40)-C(39)	119.903	O(24)-C(16)-C(15)	120.778
H(74)-C(39)-C(40)	120.702	N(17)-C(16)-C(15)	116.114
H(74)-C(39)-C(38)	119.852	H(59)-C(15)-C(19)	120.221
C(40)-C(39)-C(38)	119.446	H(59)-C(15)-C(16)	109.909
H(73)-C(38)-C(39)	119.817	H(59)-C(15)-C(13)	114.692
H(73)-C(38)-C(37)	118.736	C(19)-C(15)-C(16)	129.558

Angle	Degree	Angle	Degree
C(39)-C(38)-C(37)	121.447	C(19)-C(15)-C(13)	51.747
H(72)-C(37)-C(38)	121.13	C(16)-C(15)-C(13)	111.987
H(72)-C(37)-C(36)	119.931	H(58)-C(14)-C(19)	117.059
C(38)-C(37)-C(36)	118.938	H(58)-C(14)-C(7)	114.536
C(41)-C(36)-C(37)	119.832	H(58)-C(14)-C(5)	116.46
C(41)-C(36)-N(35)	117.045	C(19)-C(14)-C(7)	106.328
C(37)-C(36)-N(35)	123.12	C(19)-C(14)-C(5)	86.178
H(71)-N(35)-C(36)	115.159	C(7)-C(14)-C(5)	112.825
H(71)-N(35)-C(33)	114.992	H(57)-C(13)-C(15)	116.603
C(36)-N(35)-C(33)	128.155	H(57)-C(13)-C(8)	114.516
N(35)-C(33)-O(34)	128.058	H(57)-C(13)-C(4)	116.864
N(35)-C(33)-N(22)	110.458	C(15)-C(13)-C(8)	103.587
O(34)-C(33)-N(22)	121.47	C(15)-C(13)-C(4)	88.849
H(70)-C(32)-C(31)	121.009	C(8)-C(13)-C(4)	113.132
H(70)-C(32)-C(27)	119.162	H(56)-C(12)-C(11)	120.351
C(31)-C(32)-C(27)	119.829	H(56)-C(12)-C(7)	120.496
H(69)-C(31)-C(32)	119.3	C(11)-C(12)-C(7)	119.145
H(69)-C(31)-C(30)	120.485	H(55)-C(11)-C(12)	119.458
C(32)-C(31)-C(30)	120.211	H(55)-C(11)-C(10)	119.973
H(68)-C(30)-C(31)	120.082	C(12)-C(11)-C(10)	120.552
H(68)-C(30)-C(29)	120.171	H(54)-C(10)-C(11)	119.932
C(31)-C(30)-C(29)	119.745	H(54)-C(10)-C(9)	119.63
H(67)-C(29)-C(30)	120.009	C(11)-C(10)-C(9)	120.416
H(67)-C(29)-C(28)	119.404	H(53)-C(9)-C(10)	120.302
C(30)-C(29)-C(28)	120.568	H(53)-C(9)-C(8)	120.391
H(66)-C(28)-C(29)	119.85	C(10)-C(9)-C(8)	119.263
H(66)-C(28)-C(27)	120.747	C(13)-C(8)-C(9)	125.415
C(29)-C(28)-C(27)	119.401	C(13)-C(8)-C(7)	113.939
C(32)-C(27)-C(28)	120.198	C(9)-C(8)-C(7)	120.396
C(32)-C(27)-N(26)	117.401	C(14)-C(7)-C(12)	126.494
C(28)-C(27)-N(26)	122.343	C(14)-C(7)-C(8)	112.875
H(65)-N(26)-C(27)	115.522	C(12)-C(7)-C(8)	120.217
H(65)-N(26)-C(25)	109.835	H(52)-C(6)-C(5)	120.555
C(27)-N(26)-C(25)	132.946	H(52)-C(6)-C(1)	121.236
O(42)-C(25)-N(26)	122.232	C(5)-C(6)-C(1)	118.204
O(42)-C(25)-N(18)	118.356	C(14)-C(5)-C(6)	118.715
N(26)-C(25)-N(18)	119.407	C(14)-C(5)-C(4)	85.63
Cu(43)-O(24)-C(16)	130.038	C(6)-C(5)-C(4)	116.418
Cu(44)-O(23)-C(20)	127.833	C(13)-C(4)-C(5)	85.412
H(64)-N(22)-Cu(44)	69.652	C(13)-C(4)-C(3)	122.429
H(64)-N(22)-C(33)	122.227	C(5)-C(4)-C(3)	116.637
H(64)-N(22)-N(21)	115.858	H(51)-C(3)-C(4)	120.23
Cu(44)-N(22)-C(33)	116.404	H(51)-C(3)-C(2)	121.829
Cu(44)-N(22)-N(21)	102.684	C(4)-C(3)-C(2)	117.888
C(33)-N(22)-N(21)	117.677	H(50)-C(2)-C(3)	120.526
H(63)-N(21)-N(22)	113.195	H(50)-C(2)-C(1)	116.802
H(63)-N(21)-C(20)	122.137	C(3)-C(2)-C(1)	122.619
N(22)-N(21)-C(20)	118.312	H(49)-C(1)-C(6)	119.409
O(23)-C(20)-N(21)	121.699	H(49)-C(1)-C(2)	117.133
O(23)-C(20)-C(19)	121.558	C(6)-C(1)-C(2)	123.421